

ASPECTS OF THE SSR1 COLDMASS ASSEMBLING

Fermilab Summer Student Program, 2016

FRANCO DI CIOCCHIS

University of Pisa

Supervisor:

DONATO PASSARELLI

Co-Supervisor:

MATTIA PARISE

October 10, 2016

Abstract

In this paper some steps of the SSR1 coldmass assembling were analyzed. In particular, the work has focused on the lifting phase, necessary to assemble the string on its support. It will be presented the conceptual design of specific equipment needed for the examined SSR1 assembly operations. Some experimental tests were performed to validate the SSR1 alignment procedure, and the corresponding results are reported in the final section.



Contents

1	PIP-II project	2
2	Assembling procedure of SSR1 coldmass	2
3	Stiffening frame	2
4	Lifting tooling	2
4.1	Conceptual design	2
4.1.1	Structure	2
4.1.2	Lifting system	2
4.2	Structural analysis	2
4.2.1	FEM Analysis	2
5	Alignment cavity SSR1	2
5.1	Requirements	2
5.2	Alignment system	2
5.3	Mathematical model	2
5.4	Experimental tests	2
5.5	Results	2

1 PIP-II project

PIP-II project consists in upgrading the existing linear accelerator (LINAC) at Fermilab to higher energies. With the power of PIP-II, Fermilab is planning to construct and operate the foremost facility in the world for particle physics research utilizing intense beams. PIP-II will be an upgrade to the laboratory's existing facilities, providing powerful, high intensity proton beams and supplying power for neutrino experiments. The Mu2e and Muon g-2 experiments and the Long-Baseline Neutrino Facility (LBNF) will all rely on PIP-II as the source for beam. Beam acceleration in PIP-II relies on superconducting radio frequency (SRF) components, like those developed for the International Linear Collider, to accelerate beam quickly and efficiently. These cavities are highly polished, nearly perfectly shaped niobium structures tasked with generating the electric fields needed to achieve particle acceleration without creating wasted heat. A string of SRF cavities is housed in a cryomodule, where they are bathed in liquid helium to keep the cavities at the extremely cold temperature necessary for their operation. There are five types of cavities in PIP-II project:

- half-wave resonator cavities
- two types of single-spoke resonator cavities (SSR1 and SSR2)
- two types of elliptical cavities (LB 650 and HB 650)

The first superconducting accelerating section of the PIP-II linac includes eight 162.5 MHz half-wave resonator cavities and an equal number of solenoids inside a single cryomodule. The solenoids, a type of electromagnet, are used to focus the beam as it travels. The next two accelerating sections are composed of 325 MHz single-spoke resonator cavities—two SSR1 cryomodules each containing eight cavities and four solenoids, followed by seven SSR2 cryomodules with five cavities and three solenoids. The final accelerating sections are of 650 MHz elliptical cavities, one at low beta (LB650) and one at high beta (HB650). Beam in the 11 LB650 and four HB650 cryomodules is focused not by solenoids but by normal conducting quadrupole doublets located outside of the cryomodules. The PIP-II accelerator complex is planned to deliver beam in the early part of the next decade, enabling the exploration of new physics by accelerating intense particle beams

2 Assembling procedure of SSR1 coldmass

The SSR1 coldmass consists of eight single spoke resonators, operating at 325 MHz, and four superconducting solenoids in sequence C-S-CC-S-CC-S-CC-S-C. All the cavities and solenoids will be mounted on individual support posts which are in turn mounted on a full-length strongback (Fig. 1).

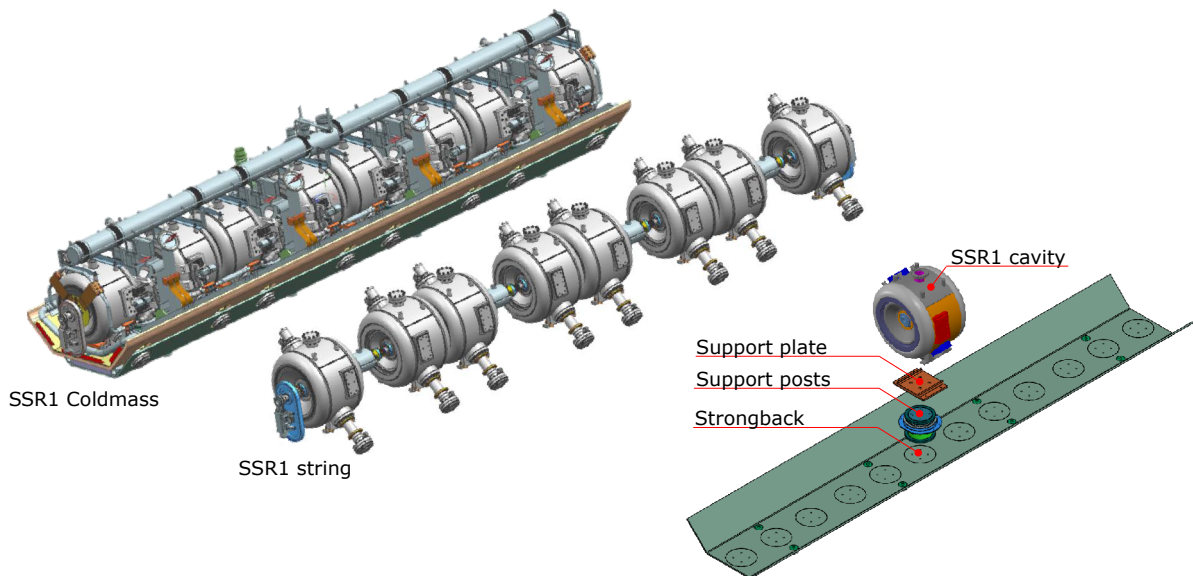


Figure 1: SSR1 Coldmass, String and main components

The SSR1 coldmass assembling is obtained through the progressive execution of different phases. In this work four main steps of the SSR1 coldmass assembling have been analyzed:

- SSR1 string assembling
- SSR1 string stiffening
- SSR1 string lifting
- SSR1 string alignment

1. In the first step the SSR1 string is assembled in the cleanroom. In this phase the string is supported by railsystem which is a specific tool designed to manipulate the string during the assembling procedure (Fig. 2).

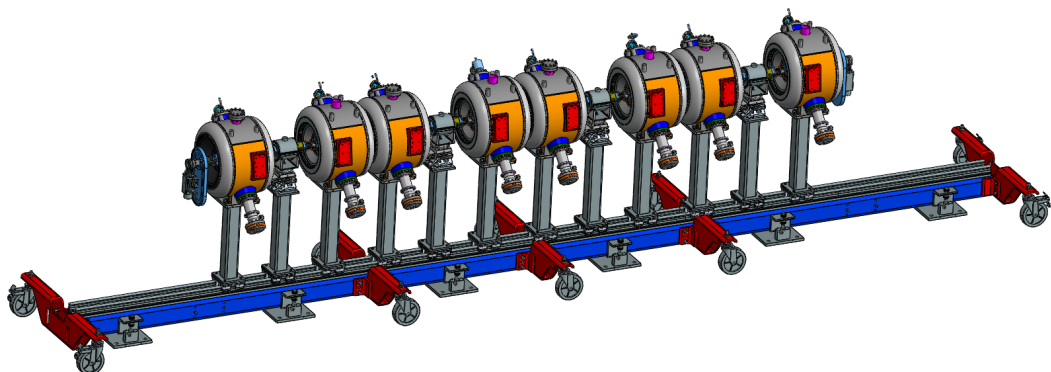


Figure 2: SSR1 string assembly

2. Since the string is not a rigid structure, it is appropriate to install a stiffening frame on it before any other operations (Fig. 3).

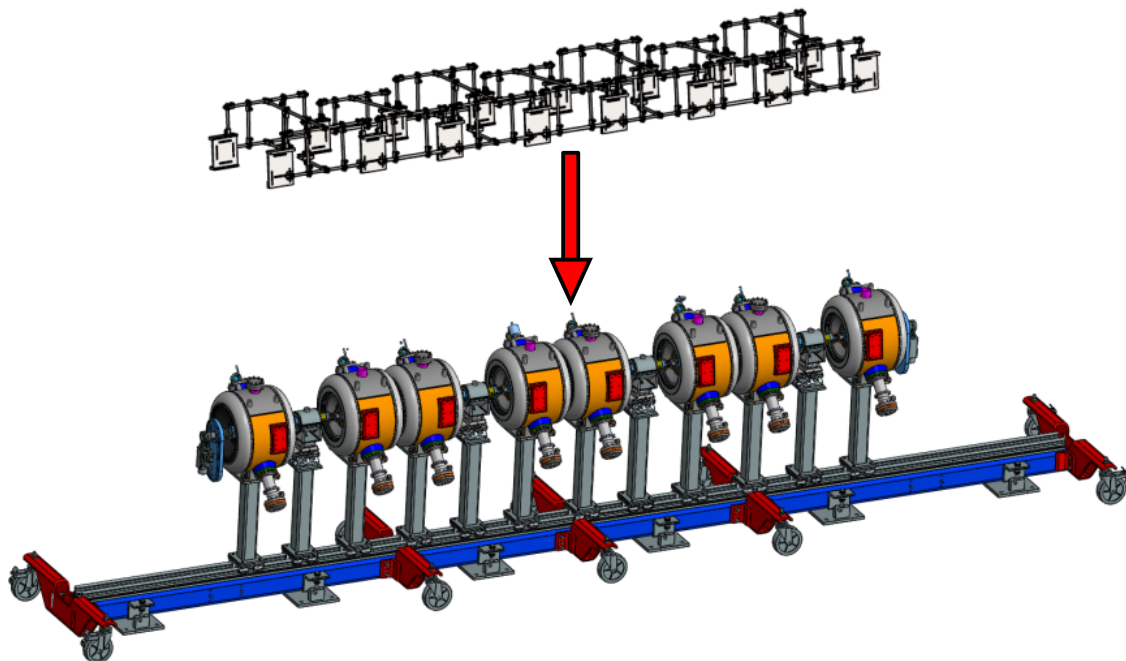


Figure 3: String stiffening operation

3. Once the string has been stiffened it is possible to move it outside the cleanroom. In the third step the string is lifted from the railsystem to be mounted on the strongback. For this operation it is necessary to develop a specific lifting device for easy and efficient transfer onto the strongback. (Fig. 4).

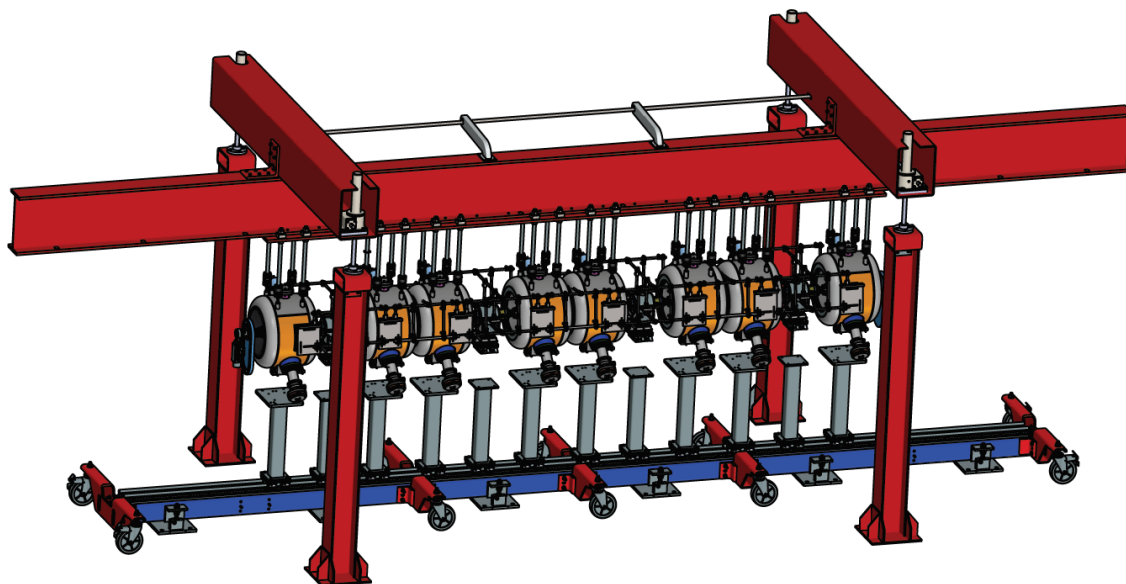


Figure 4: String lifting operation

4. Finally, when the string has been mounted on the strongback the steaffening frame must be removed and the alignment operation can be successively performed.

3 Stiffening frame

An expansion joint, commonly called bellow, is inserted between cavity-solenoid and BPM-cavity in order to compensate the thermal shrinkage (Fig. 5). This joint is designed to adsorb axial movements in a direction parallel to its axis and must not be subject to torsional load that could bring to a failure or reduce its contraction ability. For this reason, it is necessary to install an external frame on the string so as to protect itself and support the solenoids.

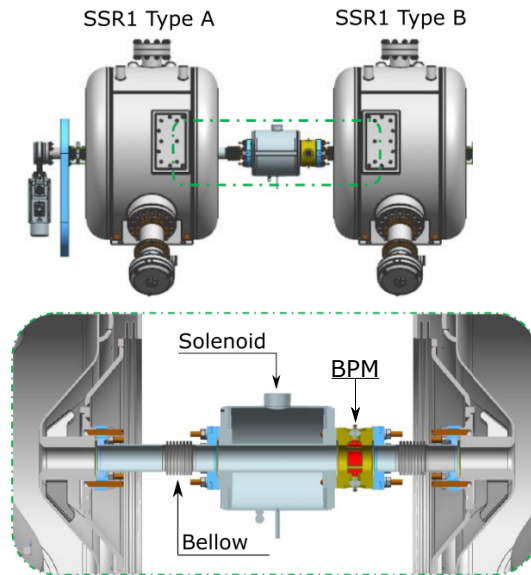


Figure 5: Interconnection cavity-solenoid and BPM-cavity

The conceptual design of the stiffening frame is a truss beam tube structure that will interface with each cavity and solenoid (Fig. 6). The tubes are interconnected using stainless steel clamps that create an adjustable system so as to eliminate any backlash in the assembly or avoid forcing on the string during the installation. Moreover, the components may be mixed and matched in a variety of configurations in order to maximize the stiffness of the structure.

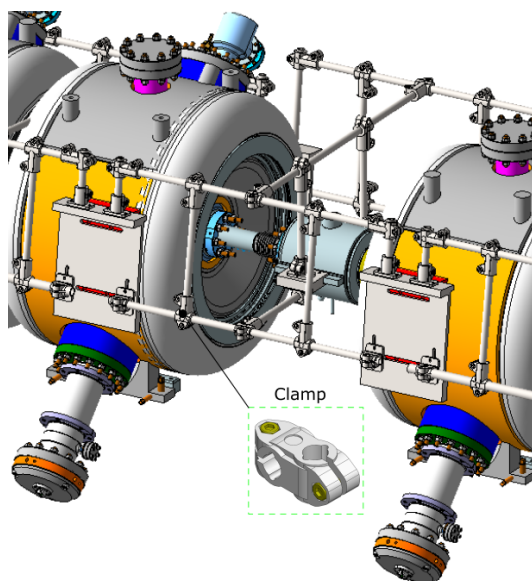


Figure 6: Stiffening frame concept

4 Lifting tooling

4.1 Conceptual design

4.1.1 Structure

In this section the conceptual design of the lifting tooling for the SSR1 and HB 650 strings is reported. The design of an appropriate structure for this operation is justified by the need of having a precise system that ensures the string integrity. In many lifting systems, ropes or chains and electric motors are used to lift the load. In this way the string could oscillate and be subjected to undesired loads, so the load should be connected to a support structure through rigid connections to prevent relative movements. The conceptual design includes a portal structure realized with standard steel beams and a mechanical lifting system (Fig. 7).



Figure 7: Lifting tooling concept

The interface with the load consists of a number of rods (four for each cavity) that will be screwed into the cavity lifting lugs (Fig. 8). A fully adjustable system can be obtained using slotted holes on the lifting beam and connecting a ball joint at the end of each rod (Fig. 9). In this way it is possible to compensate string assembling or manufacturing errors.

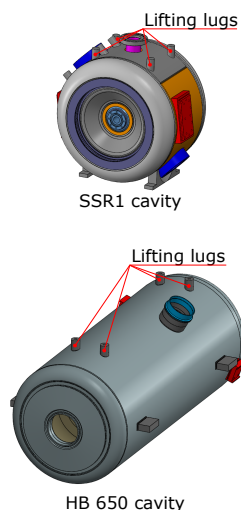


Figure 8: Cavity lifting lugs



Figure 9: Adjustable connection system

An appropriate bolted flange interface can be connected to the lifting beam in order to use the same system for both SSR1 and HB 650 strings. Moreover, all the components of the structure are interconnected using bolted joints with the aim of facilitating the assembling and the transportation of the structure.

4.1.2 Lifting system

The mechanical lifting system is made up of four worm screw jacks placed on each column and of a transmission system used for the lifting motion synchronization. In a worm screw jack, the rotation of the worm wheel acts directly on the lead screw and the lead screw translates linearly. The main advantage of jackscrews is that they are self-locking. This means that applying a torque to the shaft will cause it to turn, but no amount of axial load force against the shaft will cause it to turn back the other way, even if the applied torque is zero. Through this system the string is manually lifted by a technician who slowly rotates a lever connected to one of the screws. In order to select the size of the worm screw jacks, the total mass corresponding to the sum of the mass of the string and the one of the moving part of the structure must be considered. The worst loading configuration is the HB 650 string assembly with a mass of 1500 kg and a length of 8340 mm, while the mass of the moving part of the structure is 2000 kg. Therefore, each screw will raise a mass of 875 kg (a quarte of the total mass). The specifications of the chosen worm screw jack and gearbox are shown in [Figure 10](#).

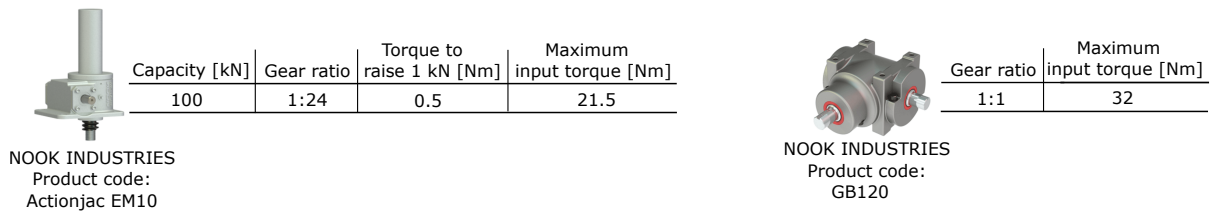


Figure 10: Worm screw jack and gear box datasheet

A complete scheme of the mechanical lifting system is reported in [Figure 11](#).

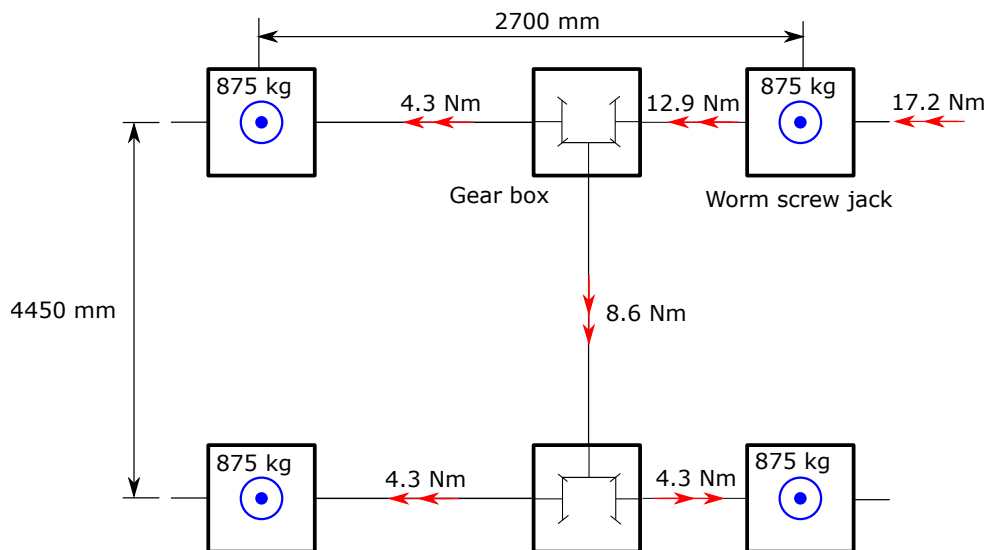


Figure 11: Mechanical transmission scheme

4.2 Structural analysis

The structure of the lifting tooling has been developed to maximize the stiffness. Excessive deformation of the beam on which the string is connected (lifting beam) could cause a string misalignment or induce undesired loads to the string. For this reason the maximum deflection of the lifting beam was limited to 1 mm. The load to be considered for this verification is the HB 650 string weight. The lifting beam cross section was estimated using the classical beam theory.

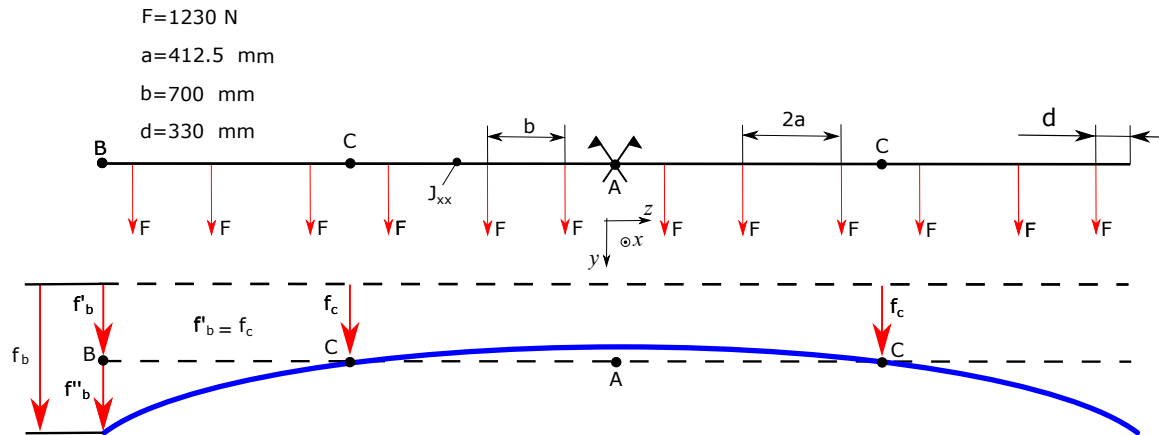


Figure 12: Lifting beam free-body diagram

The maximum lifting beam deflection can be obtained by the following relation (Fig. 12)

$$f_b'' = F \frac{640a^3 + 1152a^2b + 384da^2 + 720ab^2 + 384dab + 169b^3 + 132db^2}{48EJ_{xx}}$$

where E is the module elasticity of the material, J_{xx} the moment of inertia of the beam and F represents the half weight of the cavity. The other beams of the structure were chosen on the basis of functional specifications. The Figure 13 illustrates the main dimensions of the chosen beams cross section.

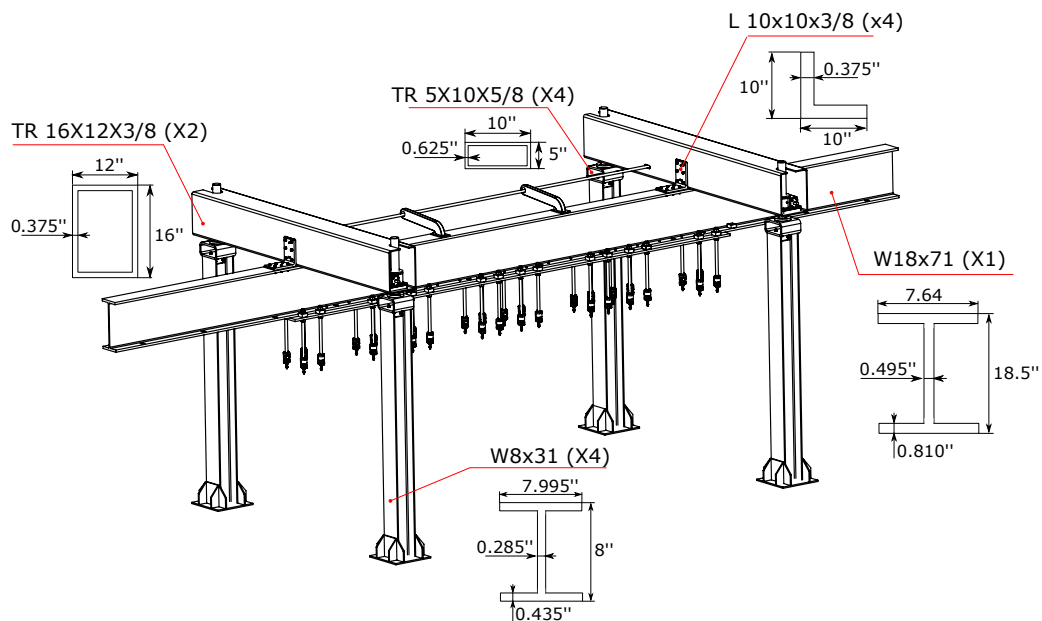


Figure 13: Conceptual structure description

4.2.1 FEM Analysis

Once a preliminary design had been performed, the structure was verified with finite element method using Ansys Workbench[®]. Taking advantage of the double symmetry, a quarter of the whole structure model was analyzed (Fig. 14). All connections were modeled using bonded contacts. In this way the analysis is linear and the computational time is significantly reduced. The weight of the structure of the lifting tooling has not been considered in the simulation; only the deformation of the structure due to the lifting operation is important to preserve the string integrity.

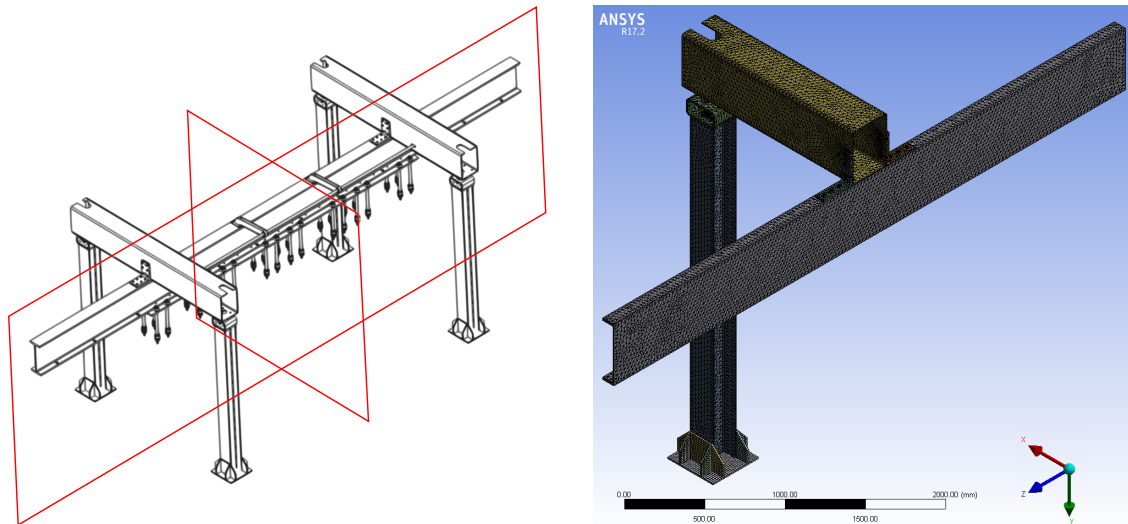


Figure 14: FEM model

The simulation results are shown in figure Figure 15.

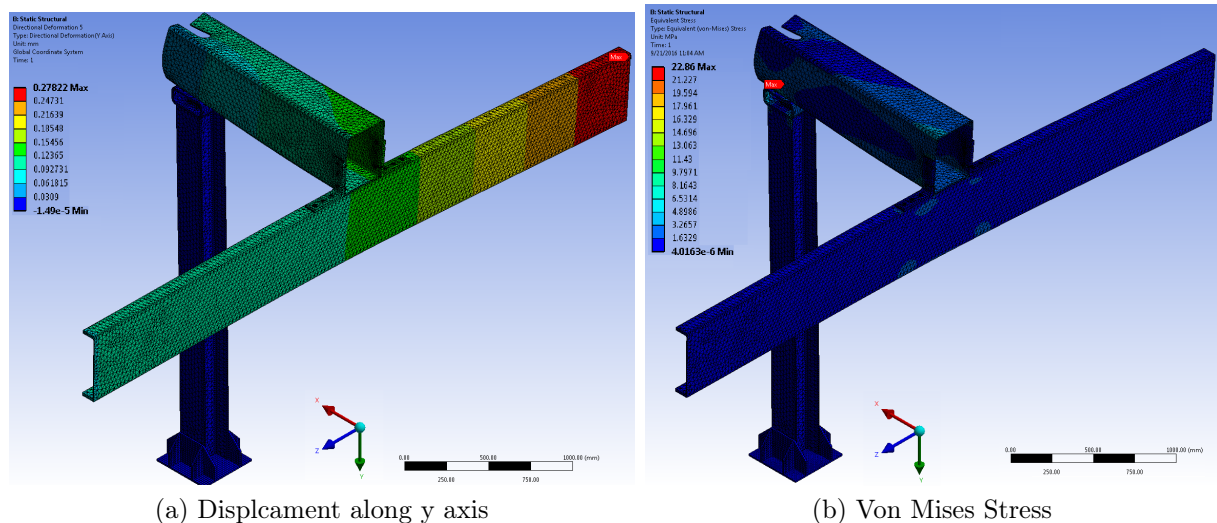


Figure 15: FEM simulation results

The structure is successfully validated with a maximum vertical displacement equal to 0.28mm . It is also clear how the structure is oversized in resistance to meet the stiffness requirements.

In order to check the accuracy of the obtained finite element method results, a convergence analysis is required. Four analyses were performed increasing the number of the elements and using the maximum displacement of the structure as a control parameter. The results are reported in [Table 1](#) and [Figure 16](#).

Analysis	n° elements	CPU time [s]	f_b
1	20750	9.4	0.195
2	30951	16	0.247
3	40492	20	0.267
4	89247	38	0.278

Table 1: Convergence analysis data

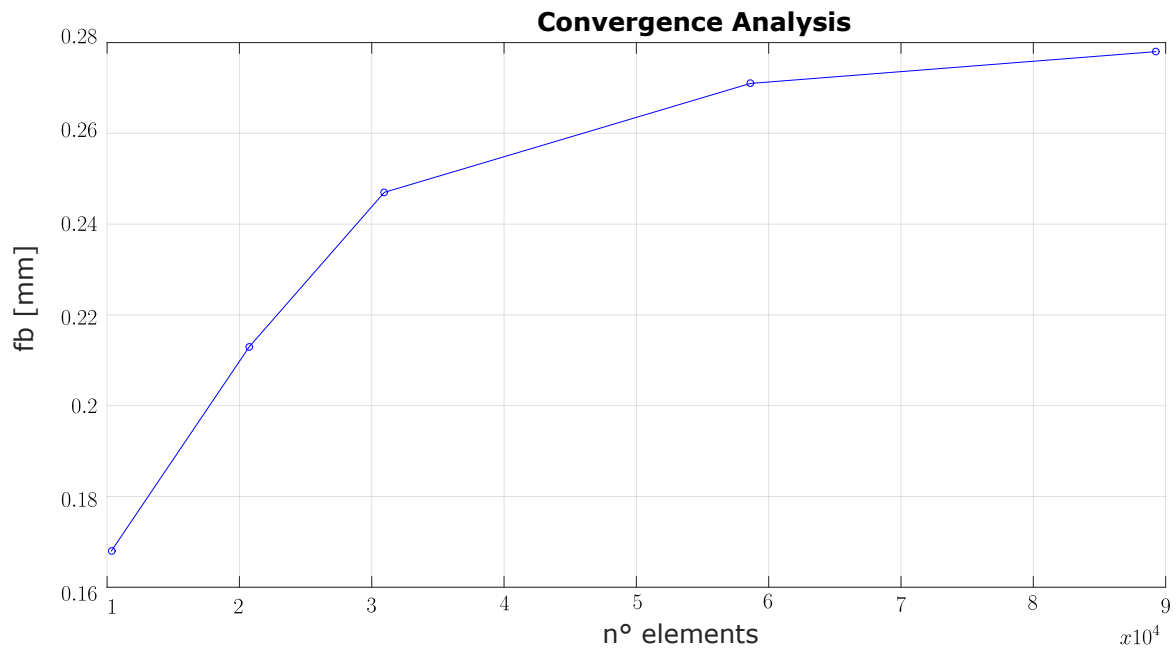


Figure 16: Convergence diagram

The diagram in [Figure 16](#) shows that a saturation is achieved when the number of the element is increased. In particular, the difference between the fourth and the third simulation is less than 4%: this means that the mesh density is adequate for this analysis and the result obtained in the fourth simulation can be considered reliable.

5 Alignment cavity SSR1

5.1 Requirements

The superconducting cavities and, especially, the magnets in high intensity proton linac need to be aligned to the beam axis within a tight range of tolerance. In the case of SSR1 cavity the maximum error allowed is $\pm 0.5\text{mm}$. The cavity must be aligned according to the geometric axis A with the help of the laser tracking technology (Fig. 17).

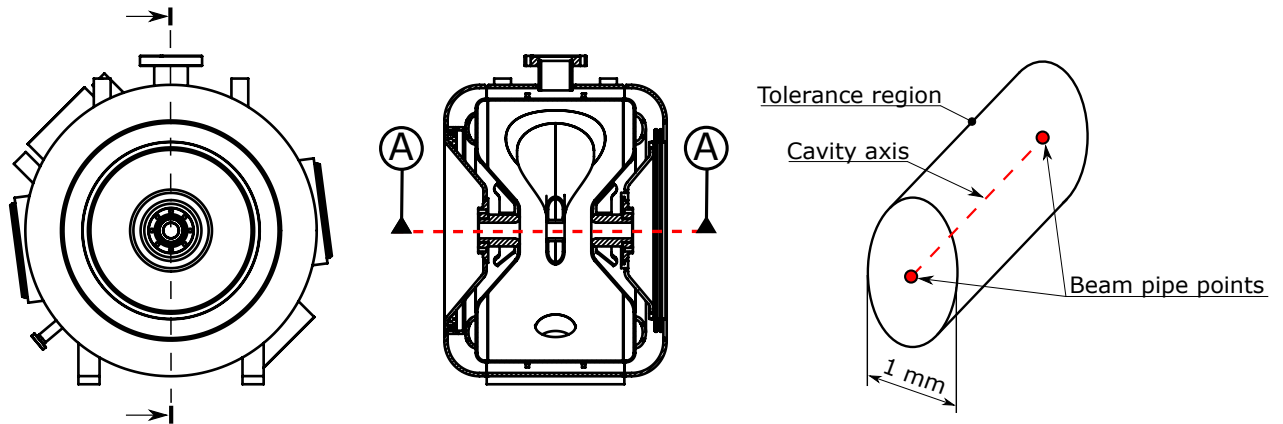
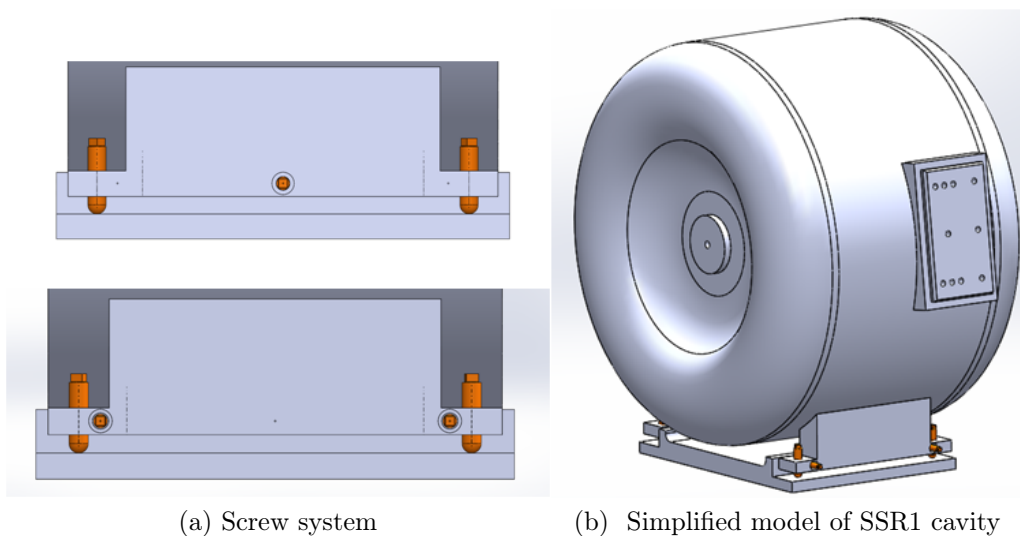


Figure 17: Reference axis and tolerance region for the alignment operation

5.2 Alignment system

The alignment system of SSR1 cavity consists of a set of seven screws inserted in two flanges welded on the cavity (Fig. 18). The tip of each screw is always in contact with the fixed reference surface. Furthermore, to reduce the friction and facilitate the alignment operation, at the tip of each vertical screw there is a spherical ball made with ceramic material. Through this system it is possible to control the orientation of the cavity and its position along two axes.



(a) Screw system

(b) Simplified model of SSR1 cavity

Figure 18: Alignment system

5.3 Mathematical model

A mathematical model was developed to simplify the alignment operation. The mathematical model is based on a serial kinematic chain commonly used in the robotic field. A serial manipulator can be schematically represented from a mechanical viewpoint as a kinematic chain of rigid bodies (links) connected by means of revolute or prismatic joints. One end of the chain is constrained to a base while an end-effector is mounted to the other end. In this case the end-effector is represented by the cavity and the reference frame has an axis aligned with the cavity axis. It is important to clarify the difference between a serial robot and a single rigid body: in a serial manipulator the end-effector configuration does not depend on the joint variable variation sequence, whereas in the rigid body case the sequence¹ of rotations influence its final orientation. For this reason it is extremely important to move the cavity, step by step, following the kinematic structure proposed.

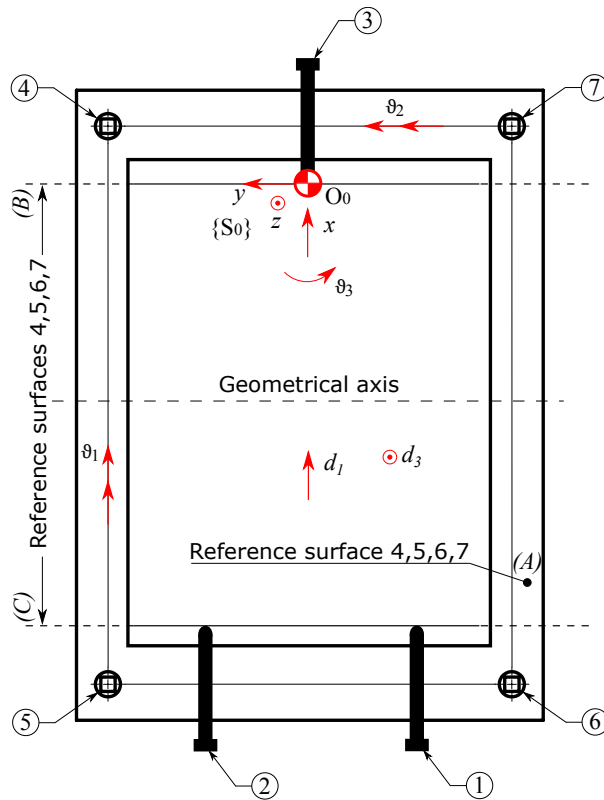


Figure 19: Screws layout

In Figure 19 the layout of the seven screws, the reference surfaces, the global frame $\{S_0\}$ and the controlled degrees of freedom are shown. Screws 1, 2 and 3 control the position of the cavity in d_1 direction and the rotation angle ϑ_3 . Screws 4, 5, 6 and 7 control the position of the cavity in d_3 direction and the angles ϑ_1 and ϑ_2 . The rotation ϑ_1 is referred to the axis passing through the contact points of the screws 4, 5; the rotation ϑ_2 is referred to the axis passing through the contact points of the screws 4, 7 and the rotation ϑ_3 is referred to the axis passing through the tip of the screw 3 and perpendicular to the reference surface (A).

¹Rotations are not commutative in three dimensions

Modeling each degree of freedom of the cavity as an idealized joint it is possible to build a serial kinematic chain. The [Figure 20](#) describes which set of the screws must be adjusted so as to obtain a specific movement of the cavity. In addition, for each degree of freedom of the cavity, a corresponding idealized joint of the serial chain is shown.

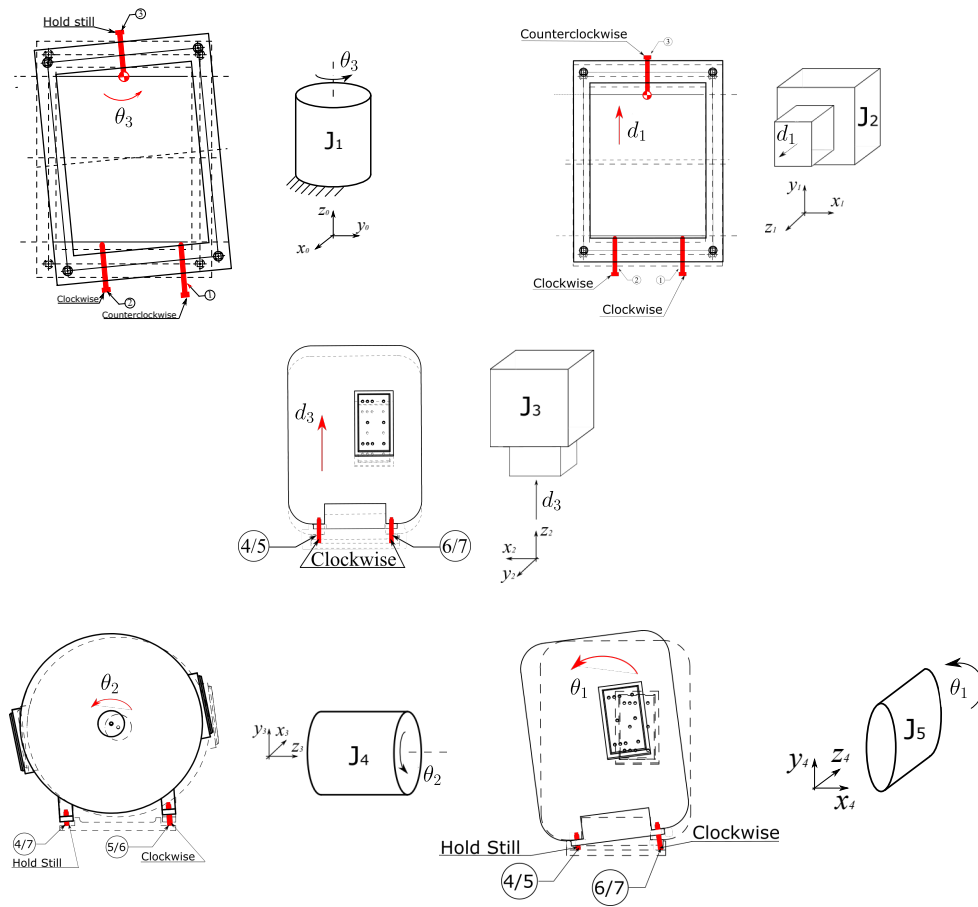


Figure 20: Procedure to control the generic degree of freedom of the cavity

The kinematic chain consists of three revolute joints and two prismatic joints corresponding to the rotations and translations of the cavity respectively ([Fig. 21](#)).

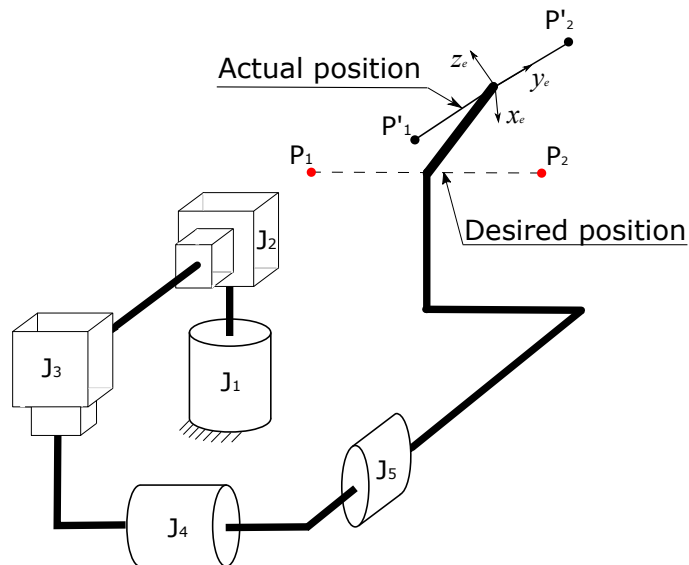


Figure 21: Complete kinematic chain

Using the inverse kinematic analysis it is possible to determine the joint parameters that provide the desired position and orientation of the end-effector. Finally, the rotation that has to be applied at each of the seven screws can be computed from simple geometric relations. The mathematical model was implemented using Mathcad[®]. The code is described by the flow chart in [Figure 22](#).

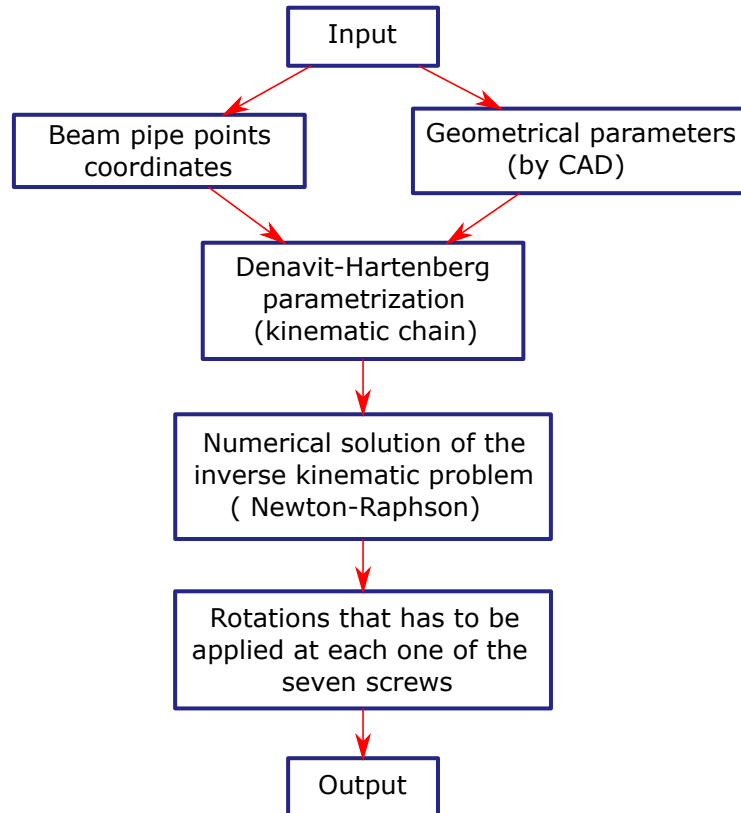


Figure 22: Mathcad code flow chart

5.4 Experimental tests

In order to validate the alignment procedure, it was necessary to assemble the SSR1 cavity on the strong-back. It was the first time that this assembly was done and not much effort was applied in mounting all the components together. The components required in the assembling are shown in [Figure 23](#).

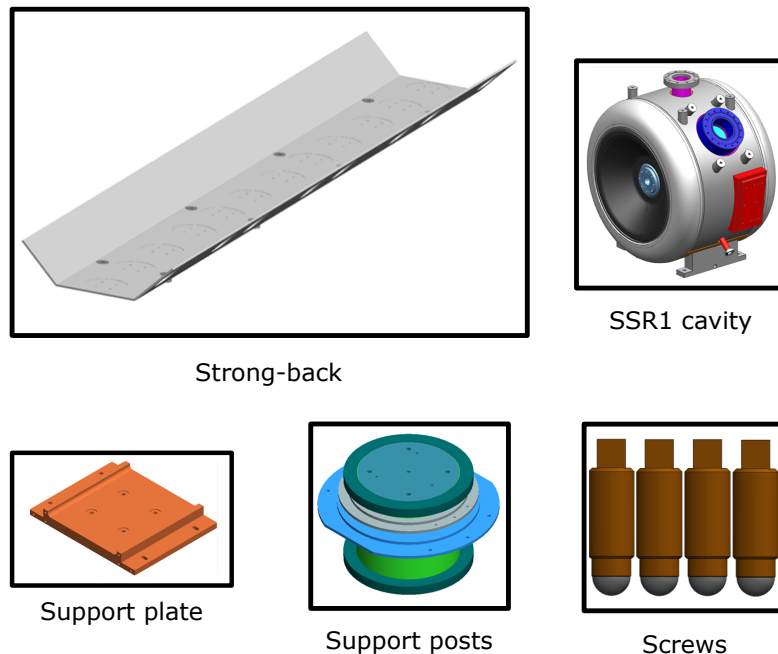


Figure 23: Necessary components

In [Figure 24](#) some phases of the assembling are shown.

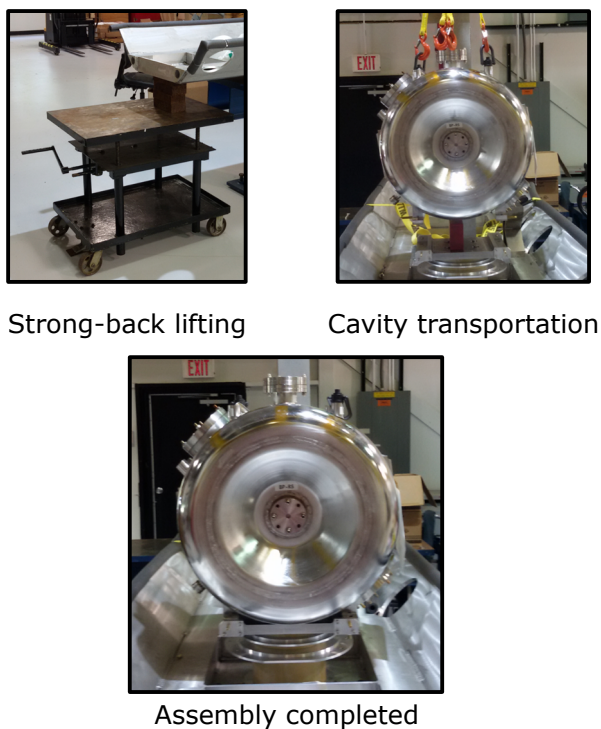


Figure 24: Main steps assembling

The purpose of these experimental tests is to validate the proposed mathematical model. The measurements were performed using analog gauges (Fig. 25), the characteristics of which are shown in Tabella 2.



Figure 25: Analog gauge

Graduations	Total Range	Range one Rev.	Stem Diameter
.0001"	.020"	.008"	.375"

Table 2: Analog gauge specifications

The gauges were placed on the tuner flanges (Fig. 26), that are related to the cavity axis. Moreover, the initial position of the gauges with respect to the cavity was obtained by caliper measurement. The measurements of the beam pipe points coordinates were not possible so, an indirect method was used.

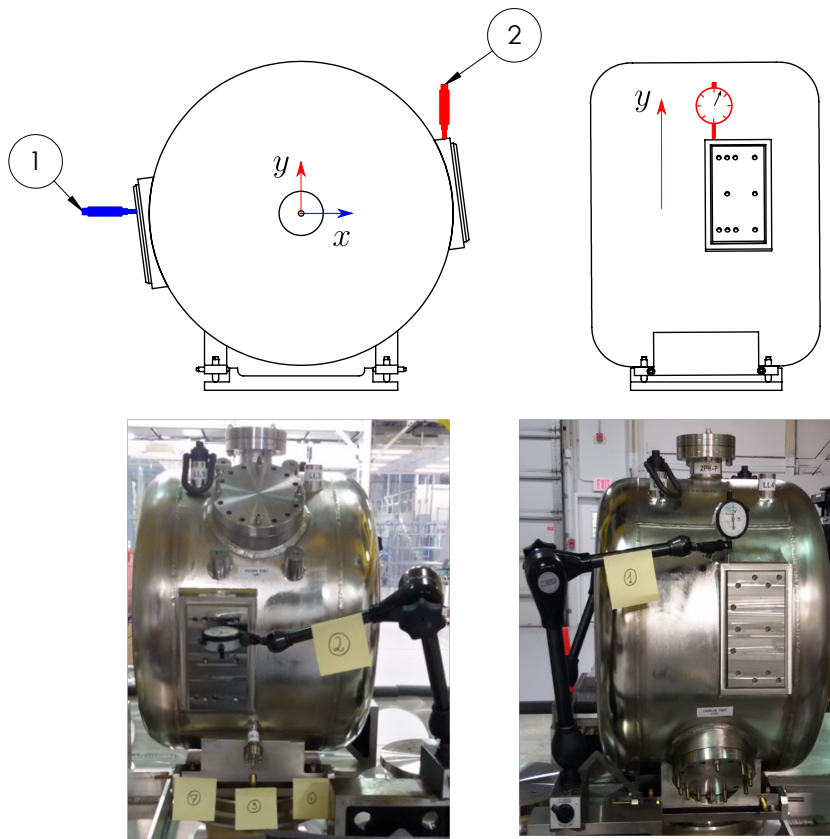


Figure 26: Setup measurements

The methodology used, with reference to a specific case, can be summarized in the following points:

1. As a first step the cavity was moved to a nominal position. In this case the rotation angles of the screws, given as output from the code, are all equal to zero, meaning that the cavity is in the desired position.
2. In the second step the screws 4 and 5 were turned 360° clockwise producing a rotation of the cavity of a certain degree amount. Once the angle of rotation is noticed, the new beam pipe coordinates can be evaluated.
3. Finally the beam pipe coordinates are given to the code as an input, and the corresponding generated outputs represent the rotation angles to be applied to each screw to return to the desired position. This should correspond to how much the screws were turned in the second step.

The produced angle of rotation of the cavity can be numerically computed (Fig. 27) from the following implicit equation:

$$2R \frac{\sin\left(\frac{\alpha}{2}\right)}{\cos(\alpha)} = \frac{\Delta_i}{\cos\left(\frac{\alpha - 2\beta}{2}\right)}$$

where

- R is the distance between the center of rotation and the initial position point of the gauge
- β is the angle that describes the position of the gauge with respect to the cavity
- α is the produced angle of rotation of the cavity
- Δ_i is the quantity measured from the i -th gauge

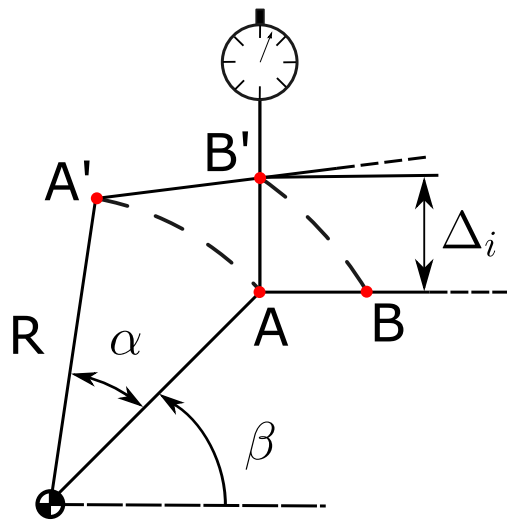
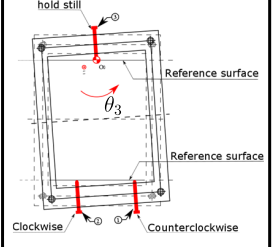
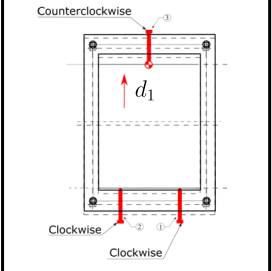
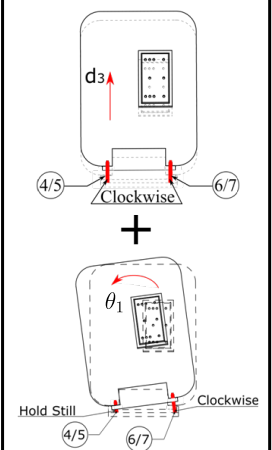


Figure 27: Quantity measured from the i -th gauge

5.5 Results

Three different tests were performed, gathering five measurements for each one. The results are shown in [Figure 28](#).

Test	Measurements	Code output															
1 360° CCW screw 1 360° CW screw 2 screw 3 fixed	<table border="1"> <thead> <tr> <th></th> <th>Δ_2 [mm]</th> <th>Average value [mm]</th> </tr> </thead> <tbody> <tr> <td>1</td> <td>0.781</td> <td rowspan="5">0.784</td> </tr> <tr> <td>2</td> <td>0.785</td> </tr> <tr> <td>3</td> <td>0.778</td> </tr> <tr> <td>4</td> <td>0.789</td> </tr> <tr> <td>5</td> <td>0.786</td> </tr> </tbody> </table>		Δ_2 [mm]	Average value [mm]	1	0.781	0.784	2	0.785	3	0.778	4	0.789	5	0.786	$AS1 = 366$ deg $AS2 = -367$ deg $AS3 := \frac{-d2\text{-mm} \cdot 360\text{-deg}}{P2} = 0$ deg	
	Δ_2 [mm]	Average value [mm]															
1	0.781	0.784															
2	0.785																
3	0.778																
4	0.789																
5	0.786																
2 360° CW screw 1 360° CW screw 2 360° CCW screw 3	<table border="1"> <thead> <tr> <th></th> <th>Δ_1 [mm]</th> <th>Average value [mm]</th> </tr> </thead> <tbody> <tr> <td>1</td> <td>1.046</td> <td rowspan="5">1.048</td> </tr> <tr> <td>2</td> <td>1.042</td> </tr> <tr> <td>3</td> <td>1.055</td> </tr> <tr> <td>4</td> <td>1.044</td> </tr> <tr> <td>5</td> <td>1.052</td> </tr> </tbody> </table>		Δ_1 [mm]	Average value [mm]	1	1.046	1.048	2	1.042	3	1.055	4	1.044	5	1.052	$AS1 = -361$ deg $AS2 = -361$ deg $AS3 := \frac{-d2\text{-mm} \cdot 360}{P2} = 361$ deg	
	Δ_1 [mm]	Average value [mm]															
1	1.046	1.048															
2	1.042																
3	1.055																
4	1.044																
5	1.052																
3 360° CW screw 4 360° CW screw 5 720° CW screw 6 720° CW screw 7	<table border="1"> <thead> <tr> <th></th> <th>Δ_1 [mm]</th> <th>Average value [mm]</th> </tr> </thead> <tbody> <tr> <td>1</td> <td>1.975</td> <td rowspan="5">1.981</td> </tr> <tr> <td>2</td> <td>1.983</td> </tr> <tr> <td>3</td> <td>1.979</td> </tr> <tr> <td>4</td> <td>1.985</td> </tr> <tr> <td>5</td> <td>1.982</td> </tr> </tbody> </table>		Δ_1 [mm]	Average value [mm]	1	1.975	1.981	2	1.983	3	1.979	4	1.985	5	1.982	$AS4 := \frac{d3\text{-mm} \cdot 360}{P1} = -354.6$ deg $AS5 := \frac{(ar1 + d3\text{-mm}) \cdot 360}{P1} = -354.6$ deg $AS6 := \frac{(ar1 + d3\text{-mm} + ar2) \cdot 360}{P1} = -719.4$ deg $AS7 := \frac{(ar1 + d3\text{-mm} + ar2) \cdot 360}{P1} = -719.4$ deg	
	Δ_1 [mm]	Average value [mm]															
1	1.975	1.981															
2	1.983																
3	1.979																
4	1.985																
5	1.982																

CW: Clockwise

CCW: Counterclockwise

Figure 28: Experimental tests results

A small difference between the code output and how much the screws were rotated can be noted. This is mainly due to manual rotation of the screws that cannot be precisely controlled. The process appears to be repeatable and the system of screws can be used to perform the alignment operation. Furthermore, if we neglect the measurement errors we can consider the mathematical model to be successfully validated.

References

- [1] LEBEDEV V. A.(2011) - *Proton Source Improvement Plan*, Beams-doc-3781-v2
- [2] RISTORI L., AWIDA M. H., GONIN I., MERIO M., PASSARELLI D. & YAKOVLEV V. (2013) - *DESIGN OF SSR1 SPOKE RESONATORS FOR PXIE*, International Particle Accelerator Conference, Shanghai
- [3] DERWENT P., HOLMES S. & LEBEDEV V. (2014) - *FNAL - THE PROTON IMPROVEMENT PLAN (PIP)*, International Particle Accelerator Conference, Dresden
- [4] SICILIANO B., SCIavicco L., VILLANI L & ORIOLO, G. (2009) - *Robotics : Modelling, Planning and Control*, Springer, 559 pp.
- [5] ROBERT C. JUVINALL & KURT M. MARSHEK (2011) - *Fundamentals of machine component design*, John Wiley & Sons Inc, 899 pp.